

AD-A127 879

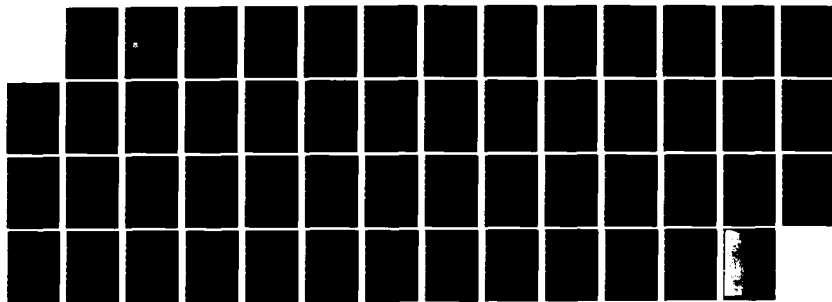
APPLICATION OF A THIRD-INVARIANT PLASTICITY THEORY TO
CONCRETE AND SOILS. (U) NEW MEXICO ENGINEERING RESEARCH
INST ALBUQUERQUE H L SCHREYER MAR 83 NMER1-8.13-TAB-25
AFML-TR-82-145 F29601-81-C-0013

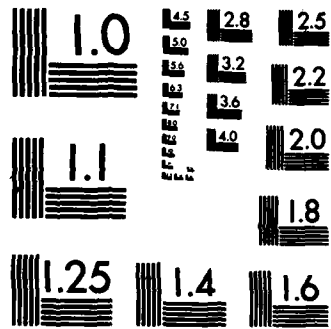
1/1

UNCLASSIFIED

F/G 8/13

NL





MICROCOPY RESOLUTION TEST CHART
NATIONAL BUREAU OF STANDARDS-1963-A

AD A135019

2

AFWL-TR-82-145

AFWL-TR-
82-145

APPLICATION OF A THIRD-INVARIANT PLASTICITY THEORY TO CONCRETE AND SOILS

Howard L. Schreyer

New Mexico Engineering Research Institute
University of New Mexico
Albuquerque, NM 87131

March 1983

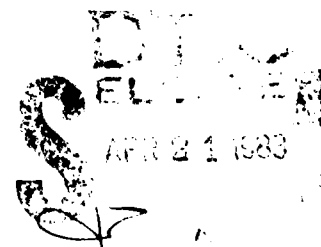
Final Report

Approved for public release; distribution unlimited.



DTIC FILE COPY

AIR FORCE WEAPONS LABORATORY
Air Force Systems Command
Kirtland Air Force Base, NM 87117



83 04 21 095

This final report was prepared by the New Mexico Engineering Research Institute, Albuquerque, New Mexico, under Contract F29601-81-C-0013, Job Order 23074201 with the Air Force Weapons Laboratory, Kirtland Air Force Base, New Mexico. Captain Terry Hinnerichs (NTES) was the Laboratory Project Officer-in-Charge.

When Government drawings, specifications, or other data are used for any purpose other than in connection with a definitely Government-related procurement, the United States Government incurs no responsibility or any obligation whatsoever. The fact that the Government may have formulated or in any way supplied the said drawings, specifications, or other data, is not to be regarded by implication, or otherwise in any manner construed, as licensing the holder, or any other person or corporation; or conveying any rights or permission to manufacture, use, or sell any patented invention that may in any way be related thereto.

This report has been authored by a contractor of the United States Government. Accordingly, the United States Government retains a nonexclusive, royalty-free license to publish or reproduce the material contained herein, or allow others to do so, for the United States Government purposes.

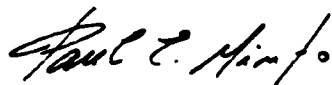
This report has been reviewed by the Public Affairs Office and is releasable to the National Technical Information Service (NTIS). At NTIS, it will be available to the general public, including foreign nations.

If your address has changed, if you wish to be removed from our mailing list, or if your organization no longer employs the addressee, please notify AFWL/NTES, Kirtland AFB, NM 87117 to help us maintain a current mailing list.

This technical report has been reviewed and is approved for publication.



TERRY HINNERICHS
Captain, USAF
Project Officer



PAUL E. MINTO
Captain, USAF
Chief, Applications Branch

FOR THE COMMANDER



JOHN H. STORM
Colonel, USAF
Chief, Civil Engineering Research Div

DO NOT RETURN COPIES OF THIS REPORT UNLESS CONTRACTUAL OBLIGATIONS OR NOTICE ON A SPECIFIC DOCUMENT REQUIRES THAT IT BE RETURNED.

UNCLASSIFIED

SECURITY CLASSIFICATION OF THIS PAGE (When Data Entered)

REPORT DOCUMENTATION PAGE		READ INSTRUCTIONS BEFORE COMPLETING FORM
1. REPORT NUMBER AFWL-TR-82-145	2. GOVT ACCESSION NO. AD-A127079	3. RECIPIENT'S CATALOG NUMBER
4. TITLE (and Subtitle) APPLICATION OF A THIRD-INVARIANT PLASTICITY THEORY TO CONCRETE AND SOILS	5. TYPE OF REPORT & PERIOD COVERED Final Report	
	6. PERFORMING ORG. REPORT NUMBER NMEPI 9.13-TA8-25	
7. AUTHOR(s) Howard L. Schreyer	8. CONTRACT OR GRANT NUMBER(s) F29601-81-C-0013	
9. PERFORMING ORGANIZATION NAME AND ADDRESS New Mexico Engineering Research Institute University of New Mexico Albuquerque, NM 87131	10. PROGRAM ELEMENT, PROJECT, TASK AREA & WORK UNIT NUMBERS 61102F/23074201	
11. CONTROLLING OFFICE NAME AND ADDRESS Air Force Weapons Laboratory (NTES) Kirtland Air Force Base, NM 87117	12. REPORT DATE March 1983	
	13. NUMBER OF PAGES 52	
14. MONITORING AGENCY NAME & ADDRESS (if different from Controlling Office)	15. SECURITY CLASS. (of this report) Unclassified	
	15a. DECLASSIFICATION/DOWNGRADING SCHEDULE	
16. DISTRIBUTION STATEMENT (of this Report) Approved for public release; distribution unlimited.		
17. DISTRIBUTION STATEMENT (of the abstract entered in Block 20, if different from Report)		
18. SUPPLEMENTARY NOTES		
19. KEY WORDS (Continue on reverse side if necessary and identify by block number) Viscoplasticity Concrete Soils Strain Rate		
20. ABSTRACT (Continue on reverse side if necessary and identify by block number) A viscoplastic constitutive model for frictional materials has been formulated. The approach is classical except that a nonassociated flow rule, and third invariants of stress and strain instead of the more conventional second invariants, are used. Theoretical and experimental results indicate good correlation for limit states and reasonable comparisons for deformations with a model that contains a small number of material parameters. Additional work is needed to improve the hardening and softening features of the model. Exploratory investigations were also conducted on the possibility of incorporating strain rate		

DD FORM 1473 1 JAN 73 EDITION OF 1 NOV 65 IS OBSOLETE

UNCLASSIFIED
SECURITY CLASSIFICATION OF THIS PAGE (When Data Entered)

UNCLASSIFIED

SECURITY CLASSIFICATION OF THIS PAGE(When Data Entered)

20. ABSTRACT (Continued)

and cracking into the model. Preliminary results indicate that for both effects it may be possible to use the existing viscoplastic framework to provide a compact but comprehensive algorithm. If an interface is modeled as an existing crack, it may also be possible to handle interaction problems with the model. The primary focus of subsequent research will involve cracking, rate effects, and interface phenomena.



UNCLASSIFIED

SECURITY CLASSIFICATION OF THIS PAGE(When Data Entered)

ILLUSTRATIONS

<u>Figure</u>		<u>Page</u>
1	Theoretical predictions for a range of rate effects and static experimental results (Ref. 1) for loose sand	8
2	Predicted strains for uniaxial tension	12
3	Predicted strains for biaxial tension with $\sigma_2 = 0.5 \sigma_1$	13
4	Predicted strains for shear with $\sigma_2 = -\sigma_1$	14

I. INTRODUCTION

The ability to predict structural response in the vicinity of a large and sudden energy source is dependent upon definition of the loads, the behavioral characteristics of the geological material surrounding the structure, the mechanism for transferring loads from the geological material to the structure, and finally the characteristics of the structure. The basic objective of this research project is to provide an improved understanding of load transferral from one medium to another or, more specifically, the modeling of structure-media (concrete-soil) interactions. However, to address this problem it is essential that good constitutive models be available for both soil and concrete. The formulation of such a model is discussed in Section II, and the research efforts that are needed to improve the model are described.

The plasticity formulation used for this study is amenable to the incorporation of rate effects in several ways. One method is described in Section III, and theoretical results for a loose sand are presented. The model shows a smooth behavior with respect to the two parameters that are used to incorporate rate effects. The approach is therefore believed to be adequate for now, especially in light of the paucity of experimental data.

This plasticity formulation involves a parameter that can be interpreted as the shear capacity of a material under zero mean pressure. With a slight modification, this parameter can be used to provide tensile cutoff. As indicated in Section IV, the algorithm is numerically stable for such an application. When this parameter is allowed to drop to zero, the incorporation of fracture into the model becomes a realistic possibility.

Concrete and many geological materials exhibit softening, a phenomenon that causes severe numerical problems because it represents a state in which the stiffness of a system ceases to be positive definite. If models such as the one described in this report are to be used in large-scale computer codes, robust and efficient algorithms must be available to handle both dynamic and static loading conditions. Static loading conditions are especially difficult; this problem is discussed briefly in Section V.

The report concludes with a brief summary of the research problems associated with this project. Also discussed in Section VI are the particular areas on which this research will focus as the work continues.

II. PLASTICITY MODEL

The current version of the plasticity model is described in Appendix A. Of particular note is the use of a new third invariant that allows the limit surface and the flow surface to be described adequately with straight lines. This formulation automatically leads to a good representation of limit stresses with smooth hardening and softening features. The model has also been used to provide comparisons for a variety of paths and materials other than those shown in Appendix A. Detailed comparisons with a weak concrete will be presented in a future report.

One of the fundamental assumptions implicit in the theory is that at the limit state, some measure of inelastic strain will assume the same value for all stress paths. The current measure involves a path length in the space of the first and third invariants of inelastic strain. It is found that, for example, predictions of strain at the limit state for uniaxial stress and pure shear are off by a factor of 2, whereas for other paths the predicted strains are within 5 percent of the experimental values. These results indicate the need for a better measure of inelastic strain, or damage, and some effort will be expended on this task. There is a distinct possibility that the use of a single measure is too simplistic and that two or more parameters will have to be used.

The use of the third invariant without the second invariant fixes the shape of the flow surface in the π -plane. The flow law is associated in this space, and for the majority of paths considered, the assumption is good. However, for certain proportional loading paths it appears that a nonassociated law may be required. An attempt will be made to identify closely the conditions under which the associativity assumption must be relaxed.

Little thought has been given to the formulation of softening within the model. However, because softening can be controlled through the relation involving the slope of the flow surface and the inelastic strain measure, alternate relations for simulating observed softening phenomena will be considered.

III. RATE EFFECTS

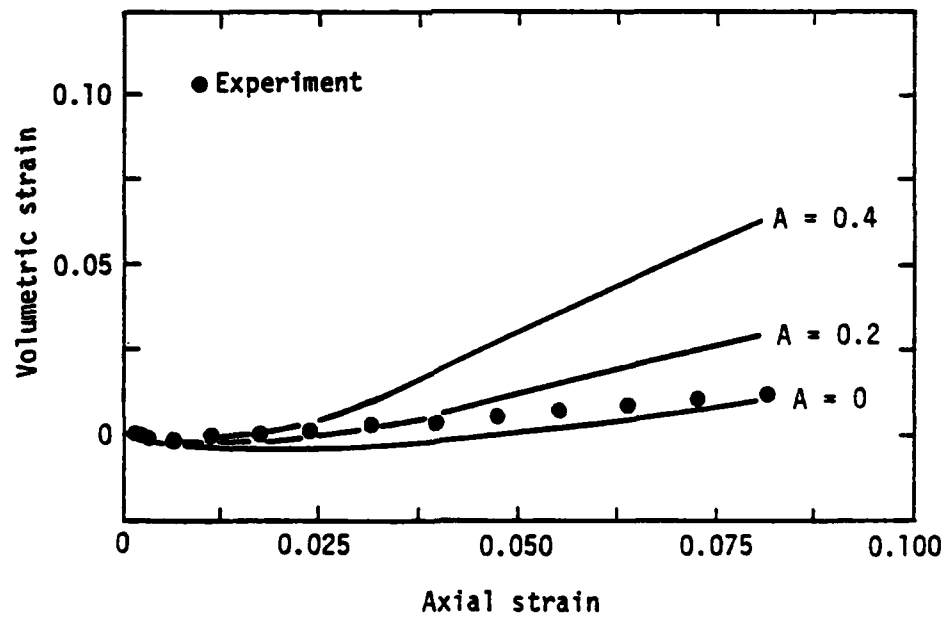
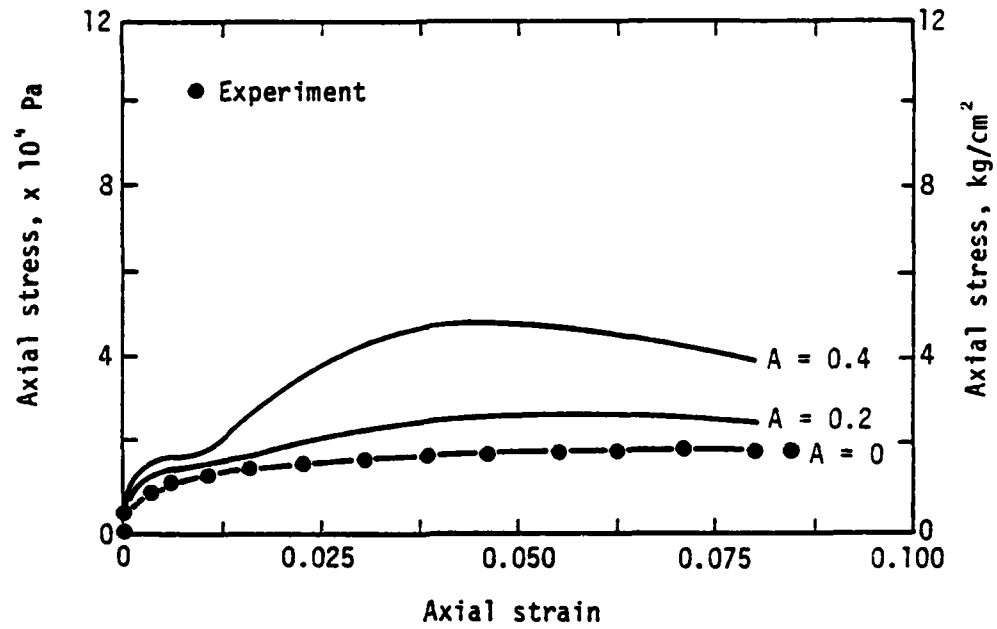
The formulation given in Appendix A is rate-independent. A conventional method of incorporating rate effects is to use an overstress approach in which the rate is related to the amount by which a measure of stress exceeds the same measure under rate-independent conditions. Thus, the strain rate is governed by the measure of stress. An alternate approach, which is the one adopted here, specifies the yield surface in terms of a measure of inelastic strain and its rate. Here, the stress is governed by the measure of strain that is used. The choice of one approach over the other is largely a matter of preference because the experimental data that would provide the basis for a selection do not exist.

The slope parameter, γ , is a function of inelastic measure of strain, $\bar{\epsilon}^i$. A viscoplastic theory is obtained if γ is replaced by a parameter, γ_r , that depends on strain rate as well. It is assumed that the following separable form is adequate:

$$\gamma_r = \gamma \left[1 - A \tanh \left(\dot{\epsilon} / \dot{\epsilon}_0 \right) \right] \quad (1)$$

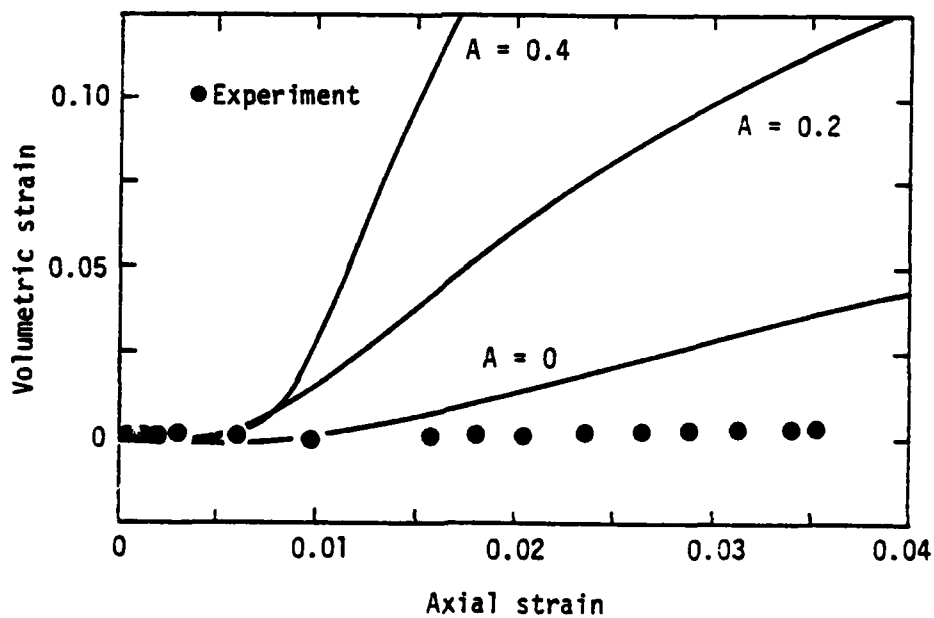
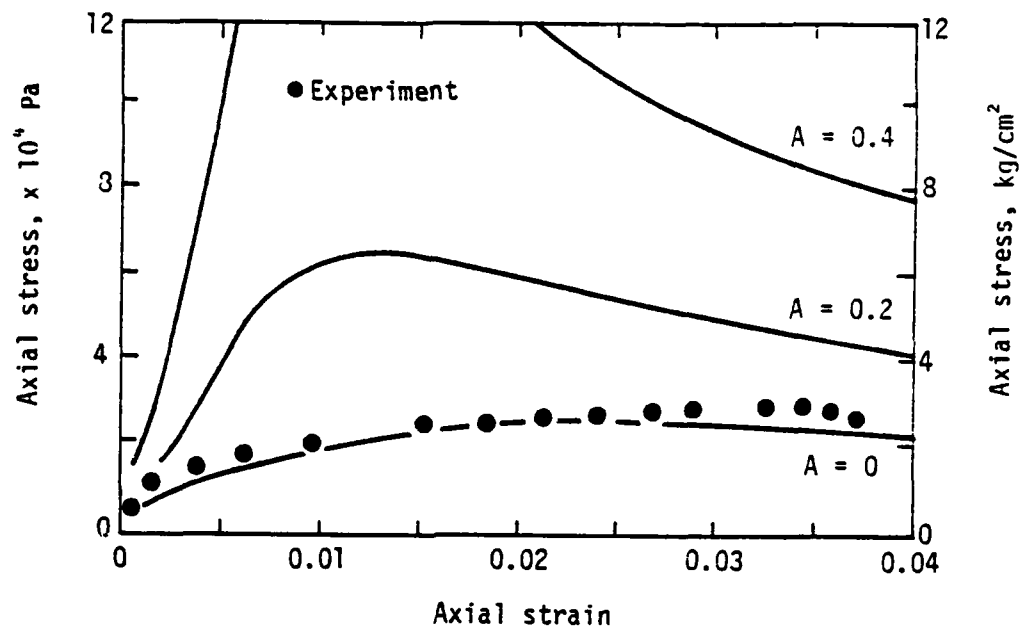
in which A is an amplification factor, $\dot{\epsilon}$ is an inelastic strain rate, and $\dot{\epsilon}_0$ denotes a reference strain rate. Sample runs were performed on a loose sand for which experimental data on the static case are available (Ref. 1). Fits to these data are shown in Figure 1 for the cases of triaxial compression and triaxial extension. These tests were performed in a cubical triaxial apparatus at constant confining stresses ($\sigma_3 = 5882$ Pa). In triaxial compression the intermediate principal stress, σ_2 , is held equal to the confining stress ($\sigma_2 = \sigma_3$), whereas in the triaxial extension test the intermediate and major principal stresses in compression are equal ($\sigma_2 = \sigma_1$). These tests represent the extreme values of the intermediate principal stress. The static comparison is good except in the case of the volumetric strain associated with triaxial extension.

A reference strain rate of 1.0 was chosen for $\dot{\epsilon}_0$, and $\dot{\epsilon}$ was arbitrarily fixed at a value of 0.75. The effect of changing A was evaluated numerically. The results are shown in Figure 1, which illustrates that the response changes smoothly with this amplification factor so that fitting experimental data



(a) Triaxial compression.

Figure 1. Theoretical predictions for a range of rate effects and static experimental results (Ref. 1) for loose sand.



(b) Triaxial extension.

Figure 1. Concluded.

should be relatively straightforward. The present formulation indicates significantly more dilatation with a strain rate effect. Whether or not this indication is realistic remains to be seen.

The only data that involve strain rates for soils in the range of interest to this study are the uniaxial strain data for a given stress rate (Refs. 2 and 3). These data will be used to evaluate parameters A and $\dot{\epsilon}_0$ as an application for the model during the next phase of this research. More effort will be expended on the formulation of a suitable experimental program that will provide the data needed for both concrete and geological materials.

IV. LIMITATIONS ON TENSILE STRESS

The existing formulation is limited to the case of positive mean pressure because not all of the implications associated with the new third invariant for tensile stresses have been investigated. However, as a preliminary investigation to determine whether the model could handle tensile cutoff, a flow rule with $\gamma = \gamma^* = 0$ or $\phi = -L - \sigma_s$ for $P < 0$ was assumed. The strains for uniaxial tension are shown in Figure 2, where the positive strain and stress axes denote compressive behavior. As the uniaxial stress is increased, the corresponding strain also increases and the lateral strains indicate contraction in the classical Poisson effect. When the cutoff stress, σ_s , is reached, the plasticity model automatically yields increasing strain with no further increase in stress, while the lateral strains remain fixed. The uniaxial strain behavior is in accordance with cracking phenomena, but the stress and lateral components of strain should drop abruptly to zero.

Predicted stress-strain behavior for a biaxial tensile path with $\sigma_2 = 0.5 \sigma_1$ is shown in Figure 3. Elastic behavior is observed until the state $L = -\sigma_s$ (which corresponds to $\sigma_1 = \sigma_s$ and $\sigma_2 = 0.5 \sigma_s$) is reached. For additional straining along the x_1 -axis, the stresses remain constant while the lateral strains exhibit a slight amount of extension. This behavior is not a good physical representation, but it may be a reasonable approximation for postcracking behavior.

A shear tensile path defined as $\sigma_1 = -\sigma_2$, with $\sigma_3 = 0$, is plotted in Figure 4. The material behaves elastically until $L = -\sigma_s$ or $\sigma_1 = \sigma_s$ and $\sigma_2 = -\sigma_s$, after which the stresses remain constant, the tensile strain continues to increase, and the other strains do not change. This is a realistic representation of physical behavior.

These examples indicate that with a minor modification to the flow surface, tensile cutoff can be represented within the existing procedure. The algorithm remains stable as one strain continues to increase in a monotonic fashion. However, the approach is too simplistic to represent cracking because most data seem to indicate that cracking is initiated when the maximum principal stress, rather than the mean stress, reaches a critical value.

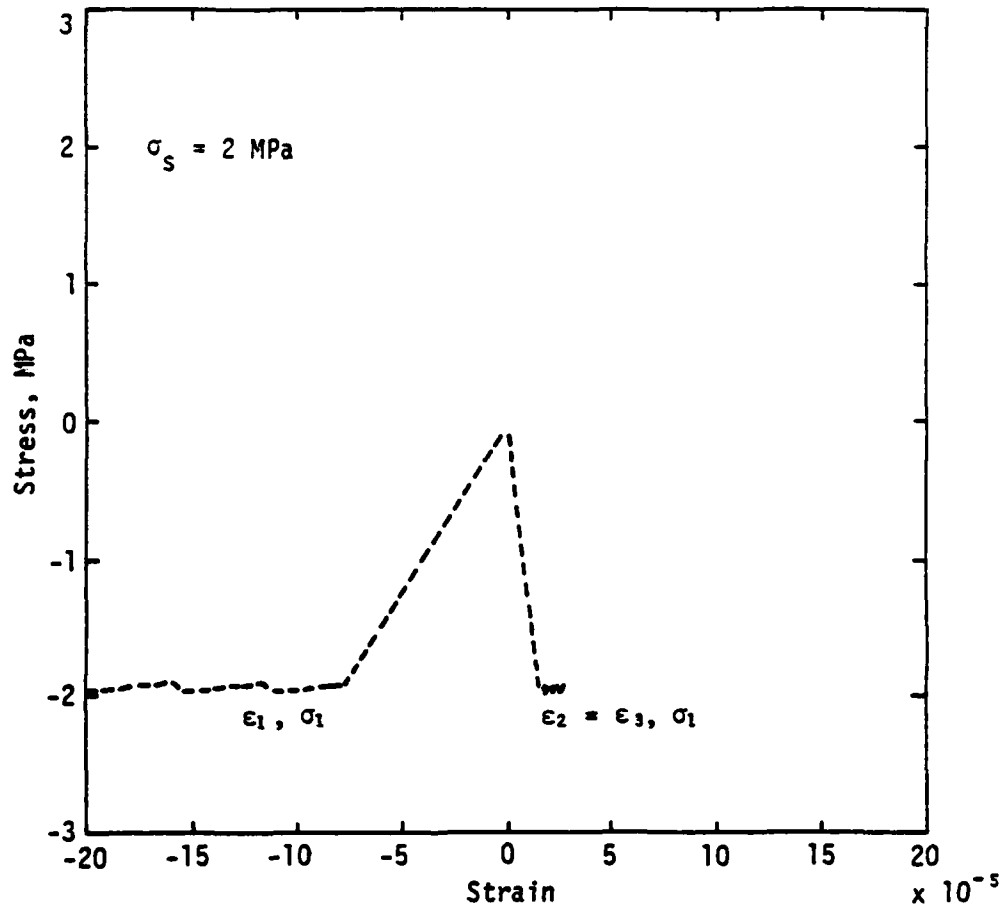


Figure 2. Predicted strains for uniaxial tension.

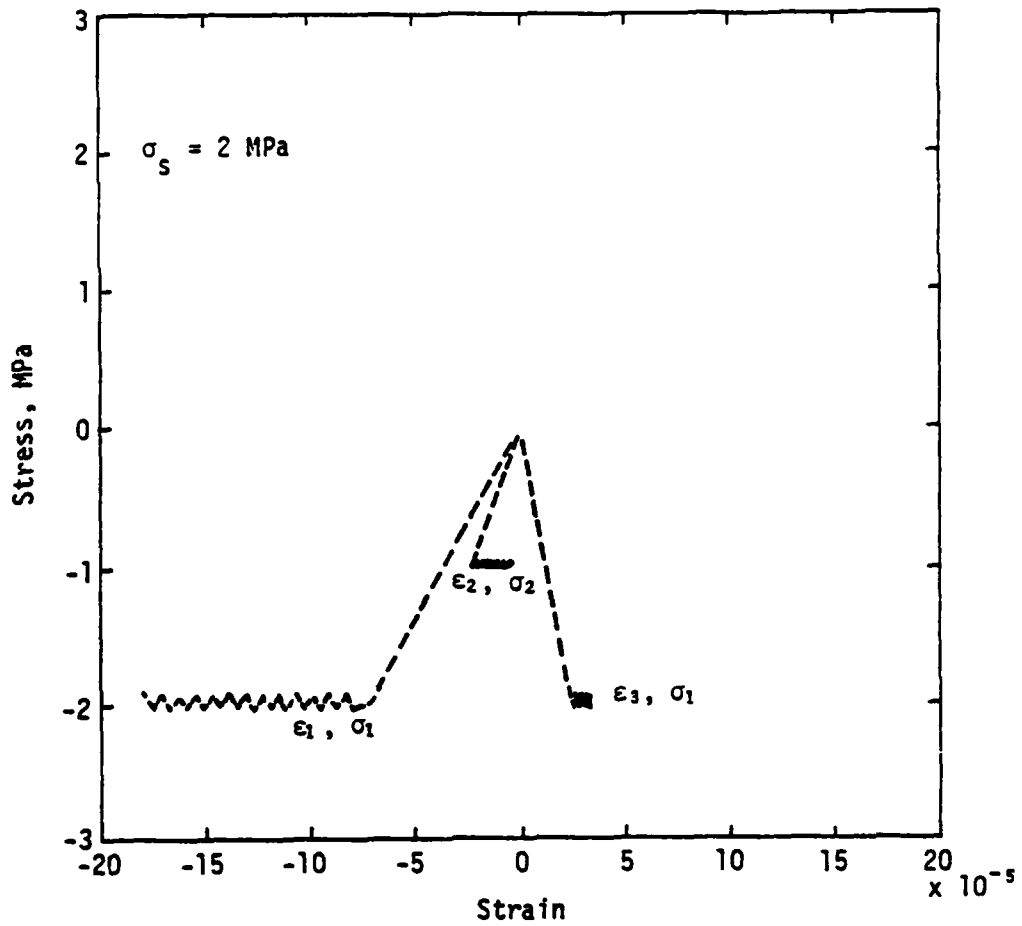


Figure 3. Predicted strains for biaxial tension with $\sigma_2 = 0.5 \sigma_1$.

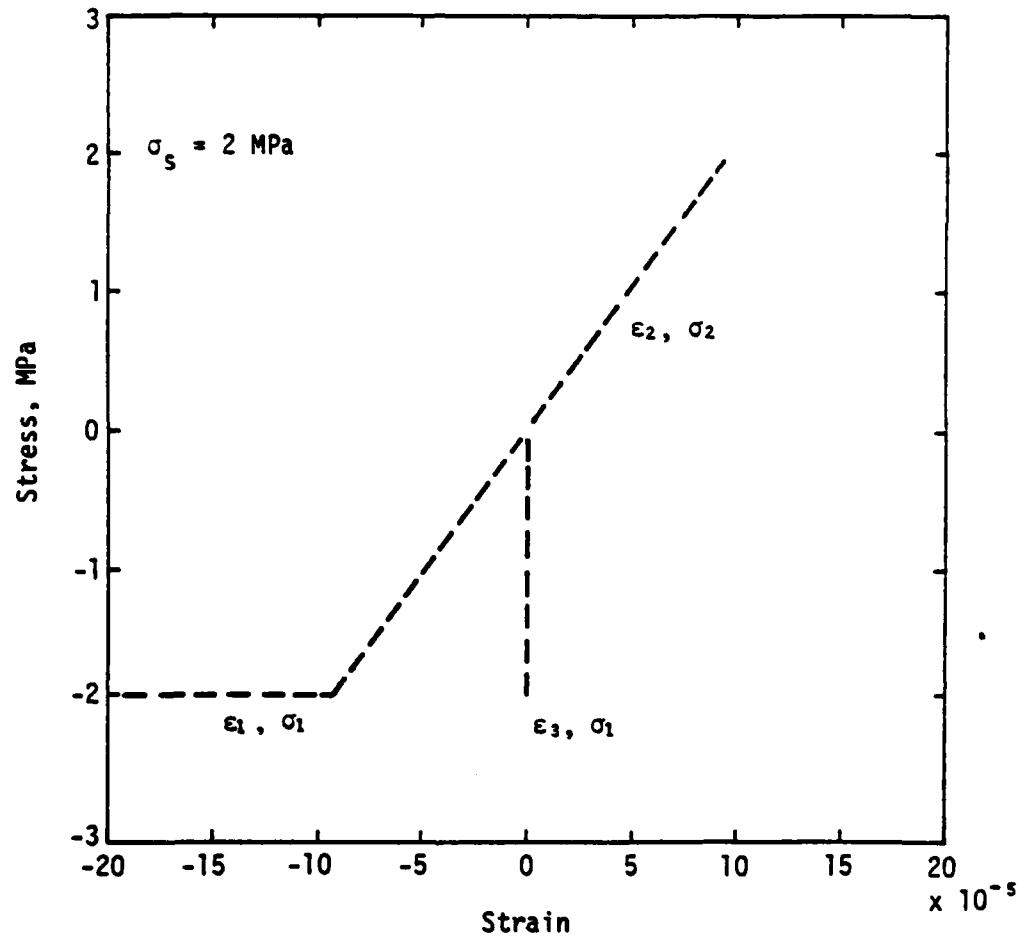


Figure 4. Predicted strains for shear with $\sigma_2 = -\sigma_1$.

The prediction of reasonable strains in the cutoff region can be attributed to the fact that the stress, σ_s , remains finite. On the other hand, a more realistic representation for stresses is obtained if σ_s drops to zero; thus, the requirements for stress and strain appear to set up conflicting demands on the model. It is believed that the issue can be handled neatly by noting that with a nonassociated flow rule, a considerable degree of flexibility is available. Thus it is proposed that the flow condition and the potential function be modified to the following forms:

$$\begin{aligned}\phi &= -L(\sigma_s) + \gamma P - \sigma_s \\ \phi^* &= -L \sigma_s^* + \gamma P - \sigma_s^*\end{aligned}\tag{2}$$

in which σ_s^* is set equal to σ_s for the beginning state. Then if a crack is predicted according to some criterion, σ_s will be reduced to zero, which will yield an appropriate stress field, while σ_s^* will be increased, which will yield an appropriate displacement field. This condition can be accomplished with very little modification to the existing algorithm.

Even this approach will not yield the directional properties associated with cracking. To obtain these properties, it is proposed that the more general form of ϕ and ϕ^* , in which the tensor $\underline{\sigma}_s$ is used instead of $\sigma_s \underline{I}$, be investigated. The questions to be answered are (1) whether the approach is feasible, and (2) if it is feasible, whether the procedure offers any advantages over the use of a cracking algorithm.

V. NUMERICAL SOLUTION PROCEDURES

A constitutive model that yields correct response features, including softening for large strains, provides a means of using less conservative designs based on the actual energy-absorbing capacity of frictional materials. These response features involve stress paths that go beyond the limit state. To predict behavior into this regime, a robust solution algorithm is required. Several exist for dynamic problems. The reason is that the mass matrix remains positive definite; consequently, it is not difficult to obtain numerical approximations to the acceleration from the equation of motion. However, the situation is quite different for softening behavior with problems that involve static loads or those that reflect transition from a dynamic to a static state. An example of the latter case is a structural member subjected to an impulse sufficiently large to force the response into the softening regime. For either case the tangent stiffness matrix ceases to be positive definite, and conventional solution procedures are no longer applicable. Alternate algorithms are available, but convergence and efficiency are matters of concern.

One approach that has considerable appeal is dynamic relaxation (Ref. 4), which is an explicit iterative method for obtaining static solutions. It is based on the fact that the static solution is the steady-state part of the transient response for a temporal-step load, and it uses the familiar dynamics equations with damping. The amount of damping is based on the critical damping factor associated with the fundamental frequency, which in turn is related to the lowest eigenvalue of the tangent stiffness matrix. If this lowest eigenvalue is zero or negative (strain softening), the damping factor is zero. For this reason the numerical solution converges very slowly under these conditions. For more conventional strain hardening, the procedure yields a solution with an efficiency similar to that obtained by using conventional matrix equation solvers.

Padovan (Ref. 5) has recently developed a procedure that involves the use of limitations on a norm of the displacement and applied load vectors.

With this measure he is able to track the local nature of the response (hardening or softening) and place suitable limitations on increments in either force or displacement to ensure accuracy and convergence. The procedure has been applied to a variety of problems (Ref. 6), but it is not clear whether the algorithm is suitable for use in a large-scale computer code. Nevertheless, the approach appears to be a distinct improvement over existing methods, and it must be considered seriously.

Quasi-Newton methods, of which BFGS is a special case, are also being applied to problems of this type (Refs. 7 and 8). These methods involve various techniques for numerically updating the Jacobian, not necessarily at every step, to provide an appropriate Newton step for minimizing a functional. Both local and global strategies are used to ensure convergence, and various steps are taken to preserve symmetry and sparsity. Also, the step size and options for backtracking are chosen for optimal efficiency. Although these concepts are still in a developmental mode as far as engineering computations are concerned, it is believed that many of them will prove to be directly applicable to engineering problems that exhibit softening.

An avenue that seems to hold considerable promise, but which apparently has not been explored, is the combination of some of the concepts of Padovan and the quasi-Newton procedures with dynamic relaxation. Because of its computational simplicity for large-scale problems and because basic equations of dynamics are used, the dynamic relaxation procedure has considerable appeal to engineers. Furthermore, it forms a natural procedure for making the transition from dynamic to static problems, even in a softening regime. Because slow convergence is a critical matter for large problems, this would seem to be a particularly productive research area in light of the need for reliable and efficient numerical algorithms.

VI. RESEARCH TOPICS

The primary aim of this project to date has been to determine the feasibility of using a simple plasticity model for frictional materials. It is believed that enough evidence has been accumulated to demonstrate conclusively that features such as strain hardening, shear enhanced compaction, dilatation, strain softening, and limit states evolve naturally from the model. An associated numerical algorithm is also functioning and appears to be reliable and fairly efficient.

The primary problem associated with the model is the accuracy of the strain predictions. For many paths, strains are within ± 10 percent of the experimental values for all stresses, which is considered more than adequate for engineering analyses involving these materials. On the other hand, predicted strains at the limit state for some paths differ from experimental values by a factor of 2. This discrepancy is not acceptable and can be attributed to the choice of a particular inelastic strain invariant. One objective of the continuing effort will be to examine closely the available experimental data in order to determine whether a better invariant can be defined. The objective is to define an invariant in such a way that the value of the invariant at the limit state is the same for all paths.

Preliminary calculations involving strain rate effects have been performed. This exploration will continue, as will the accumulation of experimental data--especially those data for multiaxial states of stress that show general trends. The objective here is to attempt to identify the functional form involving strain rates for flow surfaces that is best suited for matching experimental data. To enhance the experimental data base, an experimental program for concrete will be defined, and then a testing program will be implemented.

A potential cracking model that fits in with the plasticity formulation has been identified. If this approach should prove feasible, one constitutive relation and algorithm would handle both the compressive and the tensile

behaviors of frictional materials. The computational advantages would be considerable. Furthermore, the formulation would provide a natural framework for handling soil-structure interfaces. The anisotropic feature that is automatically present with the existence of a crack could be exploited to test postulates on how shear and normal stresses interact at an interface. Again, carefully controlled laboratory data will be sought to provide guidelines on suitable approaches.

The representation of strain softening has generally been overlooked in determining the energy-absorption capabilities of frictional materials. Because most numerical algorithms cannot cope with softening, an artificial limit stress is often used instead of the actual one. With such an approach, there is no way to accurately ascertain whether an approach is conservative, and a great deal of engineering judgment is required. Strain softening is controlled through the use of an inelastic strain invariant in the plasticity model; hence, a method of matching data is available. This aspect of the model will be explored to a limited extent to determine exactly what data are required and why.

Ultimately, any good constitutive relation will be used in large-scale computer codes. Because the plasticity model can accommodate strain softening, which is a localized feature, it becomes feasible on a modeling basis to capture softening on a global scale. One example is the response to failure of a beam subjected to a lateral load that is displacement-controlled. No currently available equation solver handles such problems routinely. The tangent stiffness method becomes singular, and the dynamic relaxation procedure is too inefficient for application to engineering problems. A numerical algorithm that could handle this problem, as well as dynamic problems, is needed. Monitoring of the literature will be continued so that new developments can be investigated as the need arises.

Although several specific topics have been addressed in this section, they are all unified around the single theme of developing accurate models for simulating soil-structure interaction. This focus will be maintained, with special emphasis on strain invariants, rate effects, and cracking.

REFERENCES

1. Lade, P. V., and Duncan, J. M., "Cubical Triaxial Tests on Cohesionless Soil," **Journal of the Soil Mechanics and Foundation Division, ASCE**, 99:793-812, 1973.
2. Jackson, J. G., Jr., Ehr Gott, J. W., and Rohani, B., "Loading Rate Effects on Compressibility of Sand," **Journal of the Geotechnical Engineering Division, ASCE**, 106:839-852, 1980.
3. Forrestal, M. J., and Grady, D. E., "Penetration Experiments for Normal Impact into Geological Targets," **International Journal of Solids & Structures**, 18:229-234, 1982.
4. Underwood, P., "Dynamic Relaxation - A Review," in **Computational Methods for Transient Response Analysis**, North Holland Publishing Co., Amsterdam, January 1983.
5. Padovan, J., and Toyichakchaikul, S., "Self-Adaptive Predictor - Corrector Algorithms for Static Nonlinear Structure Analysis," **Journal of Computers and Structures**, 15:365-377, 1982.
6. Padovan, J., and Toyichakchaikul, S., "On the Solution of Creep Induced Buckling in General Structures," **International Journal of Computers and Structures**, 15:379-392, 1982.
7. Crisfield, M. A., "Incremental/Iterative Solution Procedures for Non-Linear Structural Analysis," **Numerical Methods for Non-Linear Problems**, Proceedings of the International Conference held at University College, Swansea, September 5, 1980, pp. 261-290.
8. Pica, A., and Hinton, E., "The Quasi-Newton BFGS Method in the Large Deflection Analysis of Plates," **Numerical Methods for Non-Linear Problems**, Proceedings of the International Conference held at University College, Swansea, September 5, 1980, pp. 355-366.

APPENDIX A*

A THIRD-INVARIANT PLASTICITY THEORY FOR
FRICTIONAL MATERIALS

Howard L. Schreyer
Dept. of Mechanical Engineering
University of New Mexico
Albuquerque, NM 87131

1 October, 1982

ABSTRACT

A nonassociated plasticity theory is given for frictional materials in terms of the first and third invariants of stress and inelastic strain. Features such as strain hardening, strain softening, dilatation, and compaction are exhibited. Limit states and the Ko-condition are interpreted in a natural manner with the theory. Comparisons of predictions with experimental data for limit states and deformation paths are given for several materials.

*This appendix is a reproduction of a professional paper accepted for publication in *Journal of Structural Mechanics*. Thus, it is a self-contained document with its own internally consistent numbering system for equations, references, and figures and with a format prescribed by the publisher.

I. INTRODUCTION

The conventional theory of plasticity has a long history of successful use in applications involving metals. The theory is well-founded on a physical and a mathematical basis with numerous applications to engineering problems through the use of computer programs. This wealth of experience and familiarity has led to numerous attempts to apply the theory to frictional materials such as concrete, rock, soils, ice, and snow. Although there is no fundamental reason why the theory of plasticity should be appropriate for these materials, there are now several formulations that provide correct behavioral characteristics. Unfortunately many of these relations are so complicated that their use is limited to the simplest engineering applications. This paper is the result of an attempt to formulate a model that captures essential response characteristics without recourse to a large number of parameters or special conditions. The introduction of a new third invariant leads to a plasticity theory that appears to be natural for frictional materials in the same sense that the von Mises formulation works so well for a wide class of metals.

Drucker and Prager [1] generalized the Mohr-Coulomb hypothesis for slip to a conical yield function consisting of a linear combination of the first and second invariants. This function was then used to provide upper and lower bounds for the critical height of a vertical bank with certain implications concerning sliding surfaces and volume expansion (dilatation). This theory of perfect plasticity is too idealized to adequately represent the behavior of soils so the concept of work-hardening was applied. To account for volumetric compaction under hydrostatic loads and to control the amount

of dilatation, a cap was placed on the open end of the cone by Drucker, Gibson, and Henkel [2]. Modifications to this model have been made over the years and the fact that the approach is still in use [3] is testimony to the insight provided by these papers.

Inevitably, as more experimental data became available, the limitations of the assumed shape for the yield surface became apparent. In the π -plane the circular shape of von Mises must be replaced by a more triangular shape as expressed by the parametric form of Willam and Warnke [4]. This general shape is also obtained if the third invariant of stress is used, either directly as suggested by Lade [5] and Vermeer [6], or indirectly through the use of the Lode angle as exemplified by the work of Mroz, Norris, and Zienkiewicz [7] and Hsieh, Ting, and Chen [8]. More sophisticated versions involving multiple surfaces have been proposed [9-12] primarily to handle cyclic loading in a smooth manner consistent with experimental data. Of course, numerous rate type models have also been suggested for frictional materials [e.g., 13-15], but the requirement of a large number of material parameters has prevented their adoption to any significant scale.

The majority of these latter models are similar in that they involve all three stress invariants and that results are presented in a plane involving the first and second stress invariants. To a certain extent this has produced a degree of complexity that is not present in the original formulations of References 1 and 2. Although computers provide the luxury of accommodating several parameters, limits on storage are quickly reached for many engineering applications so that there is still a great need for formulations that capture essential response features but remain simple in form.

Lade and Duncan [16] observed that the limit state for a cohesionless soil can be represented without the use of the second invariant and Lade [17] showed recently that concrete also falls in this category. This suggests that a natural plasticity formulation for frictional materials should involve only the first and third invariants rather than all three. Lade [5] has developed this idea to a certain extent but he transforms all of his results into conventional spaces, which is done, naturally enough, to facilitate communication and comparison with previous work. However, it is believed that in attempting to use conventional concepts, the natural elegance of the theory is obscured. Here an attempt is made to present a theory in as simple a mathematical form as possible with some comparison with data to illustrate that qualitatively correct response features are obtained.

2. LIMIT SURFACES AND STRESS PATHS

Limit surfaces for concrete, rock, soils, ice, and snow depend on the first invariant of stress, or mean pressure, and are known as frictional materials in contradistinction to most metals. These surfaces also depend on a measure of shear which can be expressed through the second and third invariants of stress. The conventional approach has been to express a limit surface in terms of the mean pressure and the second invariant of the stress deviator

$$P = -\frac{1}{3} \text{tr } \underline{\underline{g}} \quad (1)$$

$$J_2' = \frac{1}{2} \text{tr } (\underline{\underline{g}}^d)^2$$

with modifications provided by incorporating a third invariant as dictated by experimental observations. Lade and Duncan [16] and Lade [17] have shown that if a particular form of the third invariant is used, the second invariant is not required in the expression for a limit surface for at least particular classes of soils and concrete. A modification of their approach is proposed to utilize this feature, which may hold for all frictional materials.

With the use of a shift in stress, $\underline{\sigma}_s$, a convenient definition for a third invariant is

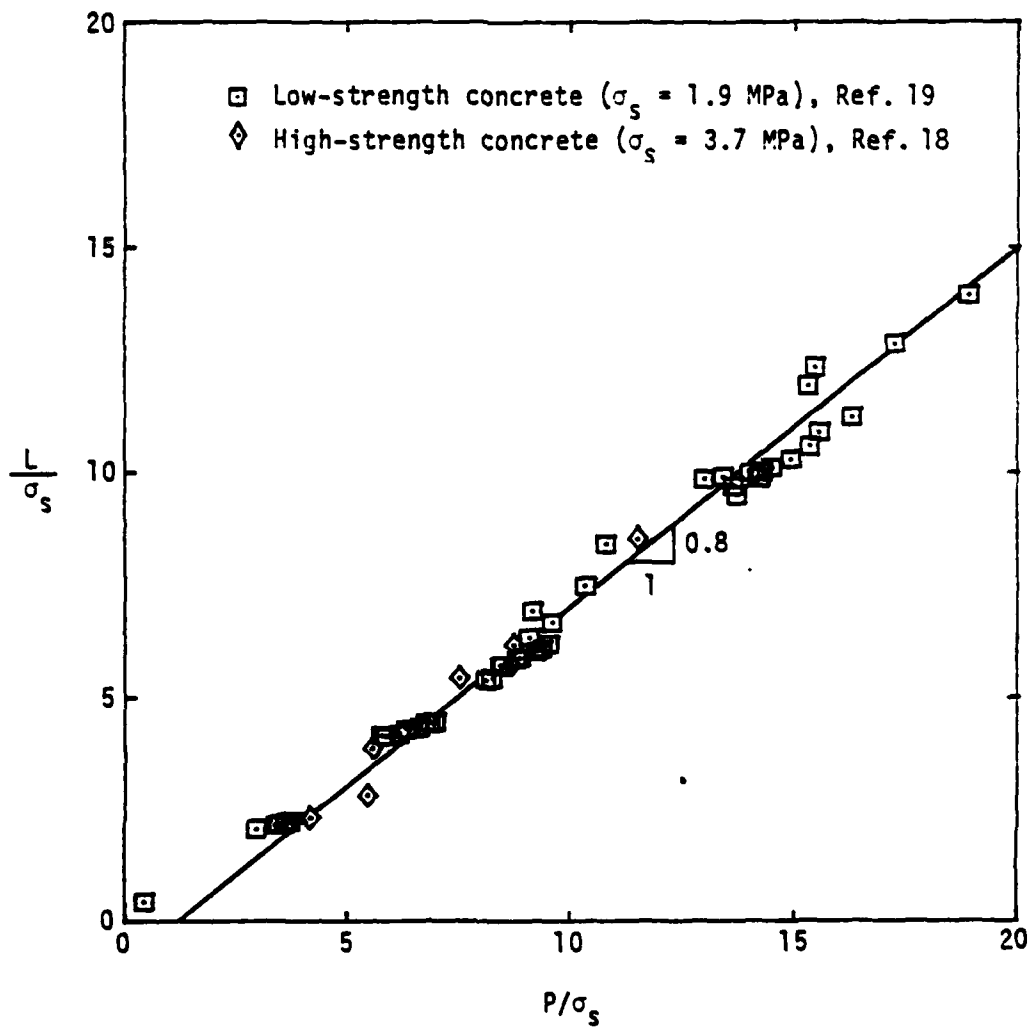
$$L = - [\det (\underline{\sigma} - \underline{\sigma}_s) + \det (\underline{\sigma}_s)]^{1/3} \quad (2)$$

in which the second term in the brackets is included to make L equal to zero for a state of zero stress. Analogous to the square root that is often used with the second invariant, a cube root is introduced to provide the dimension of stress. For principal stresses $\sigma_1, \sigma_2, \sigma_3$ and an isotropic assumption for the shift stress, $\underline{\sigma}_s = \sigma_s \underline{I}$, the first and third invariants reduce to

$$P = - \frac{1}{3} (\sigma_1 + \sigma_2 + \sigma_3) \quad (3)$$

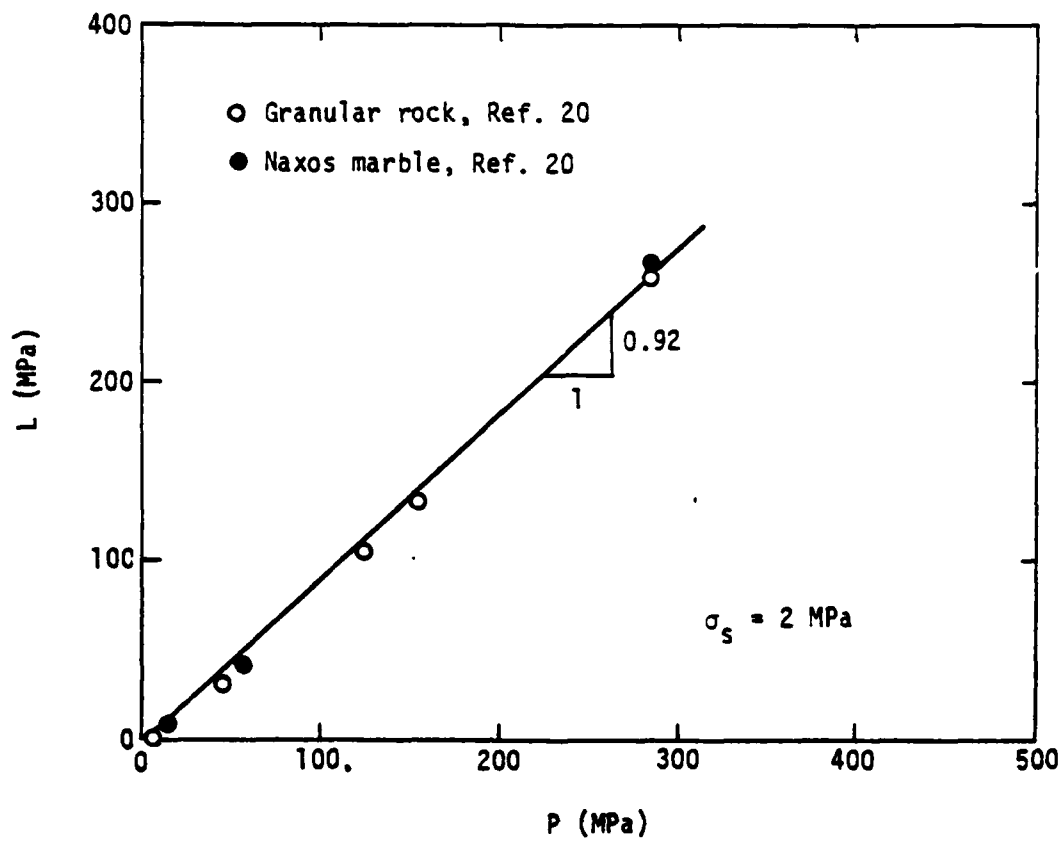
$$L = - [(\sigma_1 - \sigma_s) (\sigma_2 - \sigma_s) (\sigma_3 - \sigma_s) + \sigma_s^3]^{1/3}$$

A limit point is the point on a prescribed stress or strain path at which the state of stress is stationary with respect to increments in strain. If such points for a variety of paths are plotted in stress space, the result of interpolating between the points is a limit surface (often called a failure surface). Limit points for concrete, granite, marble, dense and loose sands, and clay are shown in Figure 1. A reasonable fit to these points is postulated to be the line



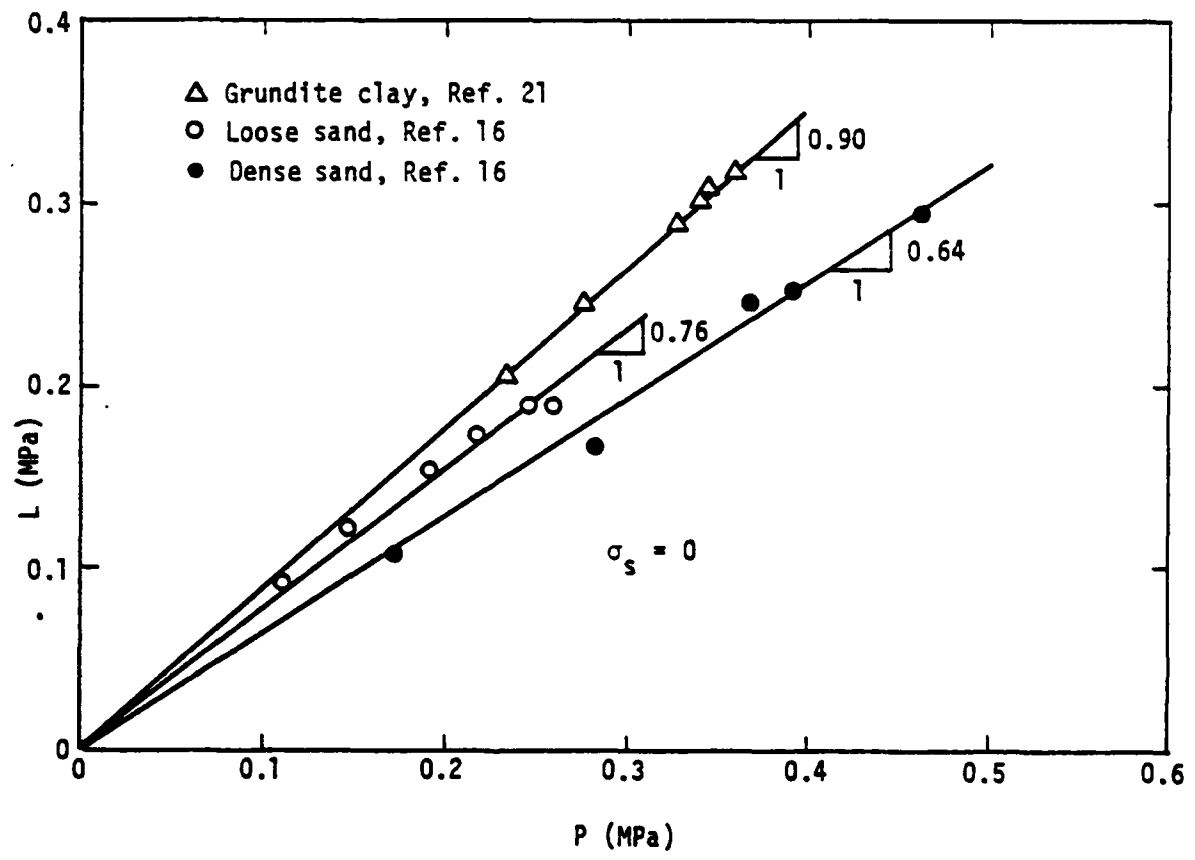
(a) Low- and high-strength concrete.

Figure 1. Limit curves for frictional materials.



(b) Granular rock and marble.

Figure 1. Continued.



(c) Clay and sand.

Figure 1. Concluded.

$$L = \gamma_L P - \sigma_s \quad (4)$$

described with two parameters consisting of a limit slope, γ_L , and the intercept on the L-axis represented by the shift stress, σ_s . The fits are remarkably good considering the elementary formulation. The scatter that is present is not unusual for these materials and indicates the need for probabilistic theory if a proper engineering analysis is to be performed.

The use of a limit surface in the P-L space suggests that this might also be a convenient space to formulate flow surfaces for use with the theory of plasticity. However, this is an unconventional space and the character of simple stress paths is not intuitively obvious. Also, there is considerable benefit to be able to relate back to other formulations and to show the potential advantages of working in this space.

In principal stress space, consider a transformation to stresses defined by

$$\begin{aligned} q_1 &= (\sigma_1 - \sigma_2)/\sqrt{2} \\ q_2 &= (2\sigma_3 - \sigma_1 - \sigma_2)/\sqrt{6} \\ q_3 &= -(\sigma_1 + \sigma_2 + \sigma_3)/\sqrt{3} \end{aligned} \quad (5)$$

The q_3 -axis defines the direction of hydrostatic pressure and the $q_1 - q_2$ plane is called the p_1 -plane. Stress paths and limit surfaces are frequently shown in the p_1 -plane and such a plot is included for the sake of completeness.

To illustrate stress paths in the P-L space, let α denote a positive, monotonically increasing parameter. Then a series of conventional load paths are defined as follows for $P \geq 0$:

(a) Hydrostatic compression

$$\sigma_1 = \sigma_2 = \sigma_3 = -\alpha$$

$$P = \alpha \quad L = [(\alpha + \sigma_s)^3 - \sigma_s^3]^{1/3}$$

$$q_1 = 0 \quad q_2 = 0$$

(b) Uniaxial compression

$$\sigma_2 = -\alpha \quad \sigma_1 = \sigma_3 = 0$$

$$P = \alpha/3 \quad L = (\alpha\sigma_s^2)^{1/3}$$

$$q_1 = \alpha/\sqrt{2} \quad q_2 = \alpha/\sqrt{6}$$

(c) Triaxial compression (hydrostatic compression to $P = \alpha_0$ followed by uniaxial compression)

$$\sigma_2 = -\alpha_0 - \alpha \quad \sigma_1 = \sigma_3 = -\alpha_0 \quad \alpha_0 > \alpha$$

$$P = \alpha_0 + \alpha/3 \quad L = [(\alpha_0 + \alpha + \sigma_s)(\alpha_0 + \sigma_s^2) - \sigma_s^3]^{1/3}$$

$$q_1 = \alpha/\sqrt{2} \quad q_2 = \alpha/\sqrt{6}$$

(d) Triaxial extension (hydrostatic compression to $P = \alpha_0$ followed by uniaxial release)

$$\sigma_1 = \sigma_2 = -\alpha_0 \quad \sigma_3 = -\alpha_0 + \alpha \quad \alpha_0 > \alpha$$

$$P = \alpha_0 - \alpha/3 \quad L = [(\alpha_0 - \alpha + \sigma_s)(\alpha_0 + \sigma_s^2) - \sigma_s^3]^{1/3}$$

$$q_1 = 0 \quad q_2 = 2\alpha/\sqrt{6}$$

(e) Biaxial compression

$$\sigma_1 = \sigma_2 = -\alpha \quad \sigma_3 = 0$$

$$P = 2\alpha/3 \quad L = [(\alpha + \sigma_s)^2 \sigma_s - \sigma_s^3]^{1/3}$$

$$q_1 = 0 \quad q_2 = 2\alpha/\sqrt{6}$$

(f) Pure shear (hydrostatic compression to $P = \alpha_0$ followed by shear)

$$\sigma_1 = -\alpha_0 + \alpha \quad \sigma_2 = -\alpha_0 - \alpha \quad \sigma_3 = 0$$

$$P = 0 \quad L_3 = -(\alpha^2 \sigma_s)^{1/3}$$

$$q_1 = 2\sqrt{\alpha} \quad q_2 = 0$$

These paths are shown in Figure 2 for $\sigma_s = 1$ and in the p_1 -plane of Figure 3.

The representation of the limit surface in the p_1 -plane is shown in Figure 3 for various values of mean pressure. For low values of P the characteristic triangle with rounded corners is obtained, and for large P the surface becomes circular, which is a feature that is generally observed for frictional materials.

Lade associates σ_s with limiting tensile behavior. The formulation here suggests an alternate interpretation. Consider the pure shear loading path with $\alpha_0 = 0$ and $\alpha = \sigma_s$. Then $L = -\sigma_s$ and, since this is a point on the limit surface (actually by design), σ_s can be interpreted as the limit stress of a material under pure shear with zero mean pressure.

A glance at the stress paths shown in Figure 2 shows that the paths fall between the hydrostatic path and the limit surface. In other words, conventional stress paths fall within a relatively narrow band in this space, which is simply a reflection of the similarity of response curves observed for this class of materials. Certain stress paths, such as triaxial compression, become almost tangent to the limit surface, so it is not surprising that experimental data for limit states show considerable scatter. For large values of P , slightly different values for γ_L yield relatively large differences in L and these differences can be magnified even further if the limit points are plotted in a different space.

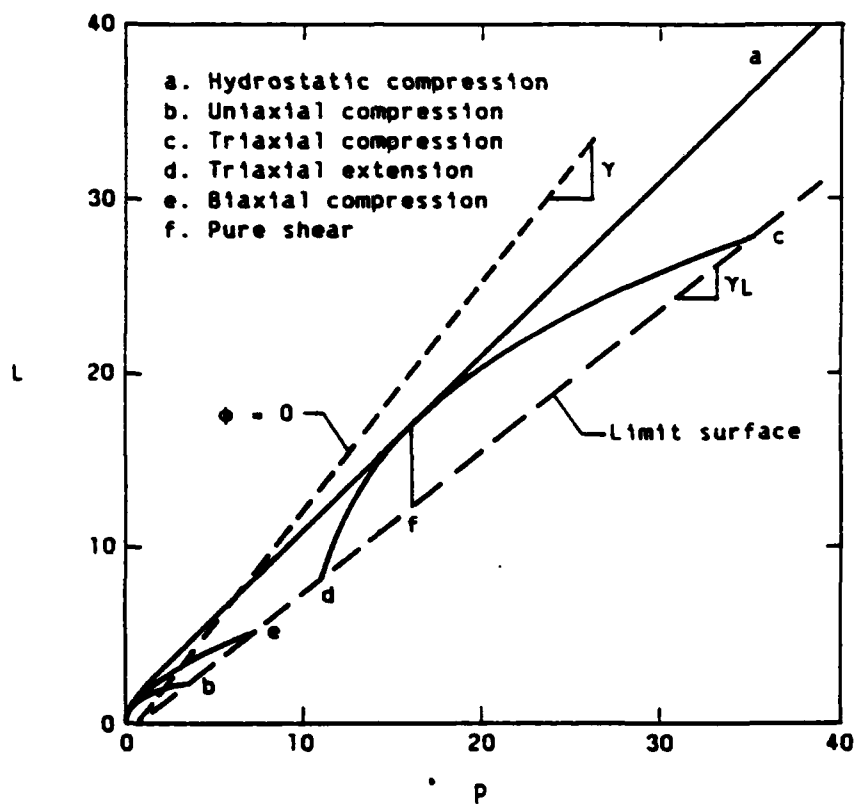


Figure 2. Stress paths and flow surfaces in the P-L plane.

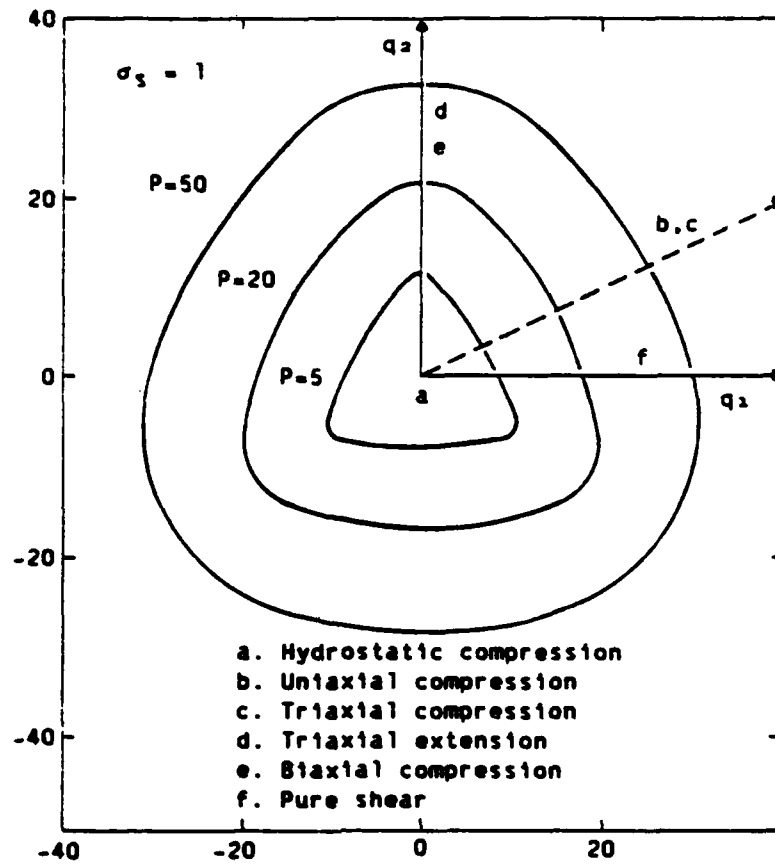


Figure 3. Stress paths and limit surfaces in the P_1 plane.

A uniaxial strain path is one of the conventional experimental paths used for soils. As the strain is increased, the lateral stresses approach a factor, K_0 , times the applied stress and this is called the "K₀ condition." In the P-L space this path depends on the material, but it is reasonable to suppose that the path asymptotically approaches the limit surface. For an applied stress $\sigma_1 = -\alpha$, and if $\alpha \gg \sigma_s$, then in the K₀ condition $\sigma_2 = \sigma_3 = -K_0\alpha$ and

$$P = \frac{\alpha}{3} (1 + 2K_0) \tag{6}$$

$$L = \alpha K_0^{2/3}$$

so that at the limit surface

$$\gamma_L = \frac{3 K_0^{2/3}}{1 + 2K_0} \tag{7}$$

The implication is that if K_0 is known for a particular material, an estimate for γ_L is available and vice versa. For example, if $K_0 = 0.40$ then $\gamma_L = 0.90$. Also, the limiting case of $K_0 = 1$, $\gamma_L = 1$ might be used to represent liquefaction.

3. FLOW SURFACES AND FLOW RULES

For the development of a plasticity relation, the initial flow surface can be developed from the point of deviation from linearity on stress-strain curves. Then this yield surface can be assumed to evolve out to a limit surface to represent the strain hardening phase of deformation. Strain softening can be obtained by letting the flow surface collapse in a controlled manner.

Since the limit surface is conveniently represented by a line in a space involving the third invariant, a flow surface of a similar nature can be postulated as follows:

$$\phi = \gamma P - L - \sigma_s \quad (8)$$

in which γ is a strain-hardening function with the restriction $\gamma \geq \gamma_L$. A surface $\phi = 0$ defines the flow state and is shown as a dotted line in Figure 2. For stress states above this line, $\phi < 0$, which represents an elastic state and $\phi > 0$ is not permitted.

A general hardening description is obtained by allowing the flow surface to rotate toward the limit line, i.e., to let γ decrease with some measure of inelastic strain to the value γ_L . Then, with further deformation, the flow surface rotates back and this represents strain softening. The specific character of a material is expressed in the functional form for γ . Some materials exhibit very little softening in which case γ would increase only slightly after reaching the limit state. Extreme softening is obtained by allowing γ to increase significantly after the limit state.

Most plasticity formulations for frictional materials are presented in terms of the first and second invariants of stress. For convenient comparisons, the flow surface of Equation (8) is shown in Figure 4 for $q_2 = 0$ and various values of γ . For $\gamma > 1$ rather conventional elliptical shapes are automatically obtained together with a general hardening behavior that would be extremely difficult to develop in the $P - \sqrt{J_2}$ plane. This is another example that indicates that the use of a third invariant is natural for frictional materials. For large P the slope of the hydrostatic path is unity, so if $\gamma > 1$ the flow surface does not intersect the hydrostatic path. This is reflected as a curve in the $p - \sqrt{J_2}$ plane that does not inter-

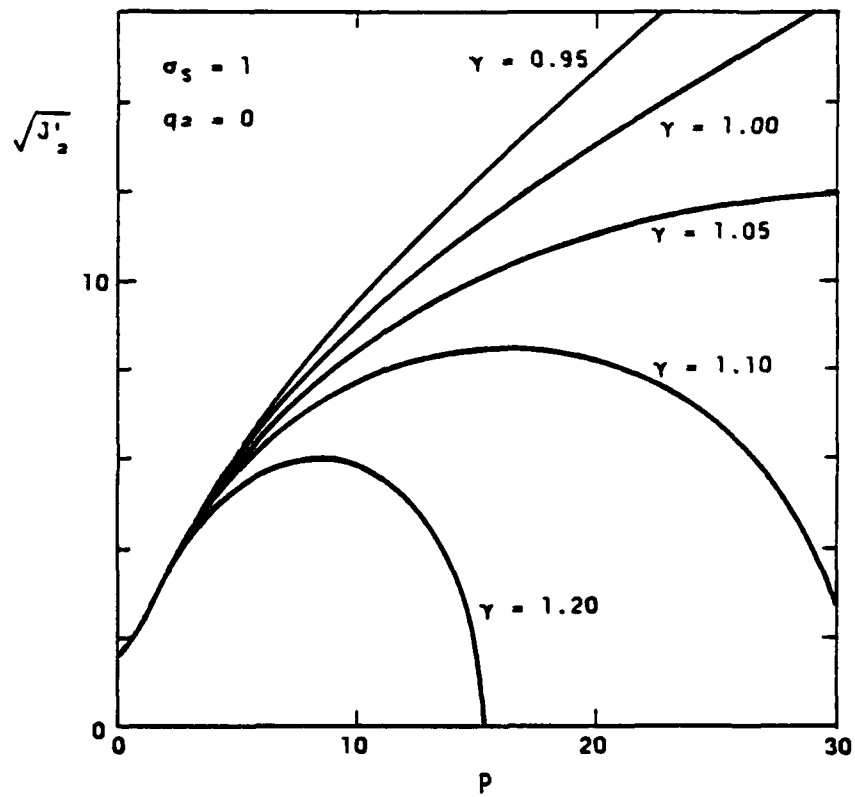


Figure 4. Flow surfaces in the $P-\sqrt{J_2}$ plane.

sect the P-axis and is a consequence of the simplest possible assumption that the flow surface is a straight line in the P-L plane.

One of the fundamental difficulties with a plasticity formulation is that appropriate measures of deformation must be selected for use in a strain hardening law. If these measures are chosen to be the inelastic strain tensor, \underline{e}_1 , then the theory is usually too complicated to be of much practical use, so a positive definite invariant, \bar{e}^{-1} , is often adopted. If a reference value, \bar{e}_o^{-1} , can be associated with a limit state for all paths, a hardening law that provides the appropriate characteristic features is given by

$$\gamma = \gamma_o - (\gamma_o - \gamma_L) \sin \frac{\pi}{2} \left(\frac{\bar{e}^{-1}}{\bar{e}_o^{-1}} \right)^n \quad (9)$$

where γ_o is the value of γ that defines the initial yield surface. The exponent, n , merely controls the rate at which γ changes with \bar{e}^{-1} .

In metal plasticity, \bar{e}^{-1} is often chosen to be the path length associated with the second invariant of the inelastic strain deviator. Here, both volumetric and shear effects are important, so it is postulated that an appropriate invariant is a path length involving all three invariants:

$$\bar{e}^{-1} = \int_0^s \left[|de_v^i| + b_2 de_2^i + b_3 de_3^i \right] \quad (10)$$

where s is a monotonically increasing load parameter, b_2 and b_3 are material constants, and

$$\begin{aligned} de_v^i &= \text{tr} (d\underline{e}^i) \\ de_2^i &= \left[\text{tr} (d\underline{e}^{id} d\underline{e}^{id}) \right]^{1/2} \\ de_3^i &= |\det(d\underline{e}^i)|^{1/3} \end{aligned} \quad (11)$$

represent inelastic volumetric and shear increments based on the inelastic strain tensor and its deviator, e^{1d} . Such a formulation has proved to be useful, at least for particular cases of sand and concrete, but it must be considered as a preliminary form for illustrative purposes.

If an associated flow rule is adopted, then

$$d \underline{e}^1 = d \lambda \frac{\partial \phi}{\partial \underline{\sigma}} \quad (12)$$

for a monotonically increasing parameter λ with the increment $d\lambda$ obtained by satisfying the consistency condition, $\phi = 0$. However, in agreement with many other investigators, such a flow rule yields an excessive amount of dilatation, so the use of a potential function, ϕ^* , instead of ϕ is required in Equation (12). After an investigation of several stress paths, a modification to γ was deemed sufficient and hence

$$\phi^* = \gamma^* P - L - \sigma_s \quad (13)$$

was chosen with the nonassociated parameter γ^* given by the simple additive relation

$$\gamma^* = \gamma + b_1 \quad (14)$$

where the constant b_1 depends on the material. The implication of Equation (13) is that the flow rule is associated with respect to L but not with respect to P .

In terms of principal stresses, the flow law yields the following expression for the inelastic volumetric strain increment:

$$d e_v^1 = \frac{d\lambda}{3L^2} \left[(\sigma_1 - \sigma_s)(\sigma_2 - \sigma_s) + (\sigma_2 - \sigma_s)(\sigma_3 - \sigma_s) + (\sigma_3 - \sigma_s)(\sigma_1 - \sigma_s) - 3L^2 \gamma^* \right] \quad (15)$$

The value of γ^* that gives the transition point between dilatation and compaction is found by satisfying the condition $d e_v^i = 0$. For example, under uniaxial compression with the stress parameter α defined previously, this value is

$$\gamma_t^* = \left(\frac{\sigma_s}{\alpha} \right)^{2/3} \left(1 + \frac{2}{3} \frac{\alpha}{\sigma_s} \right) \quad (16)$$

and if $\alpha \gg \sigma_s$, then

$$\gamma_t^* = \frac{2}{3} \left(\frac{\alpha}{\sigma_s} \right)^{1/3} \quad (17)$$

which provides some general guidance as to how the function γ^* should behave if experimental data are available for the path. For hydrostatic compression, $\gamma_t^* = 1$, and since compaction is always observed for such a state, the restriction $\gamma^* > 1$ is imposed in Equation (14).

Additional insight into the required behavior for γ^* is obtained by considering uniaxial strain. Since compaction is obtained for this path, γ^* must be greater than γ_t^* . However, at the K_0 condition, the slope of the mean pressure-volumetric strain curve is very steep which implies very small increments in inelastic deformation. Since the uniaxial strain component equals the volumetric strain for this case, γ^* must be greater than but close to γ_t^* . The use of the K_0 stress state and Equation (15) yields

$$\gamma_t^* = \frac{2 + K_0}{3K_0^{1/3}} \quad (18)$$

which gives $\gamma_t^* = 1.09$ for $K_0 = 0.4$. This is the type of information that is useful for determining the parameters b_1 , b_2 and b_3 .

4. COMPARISON WITH EXPERIMENTAL DATA

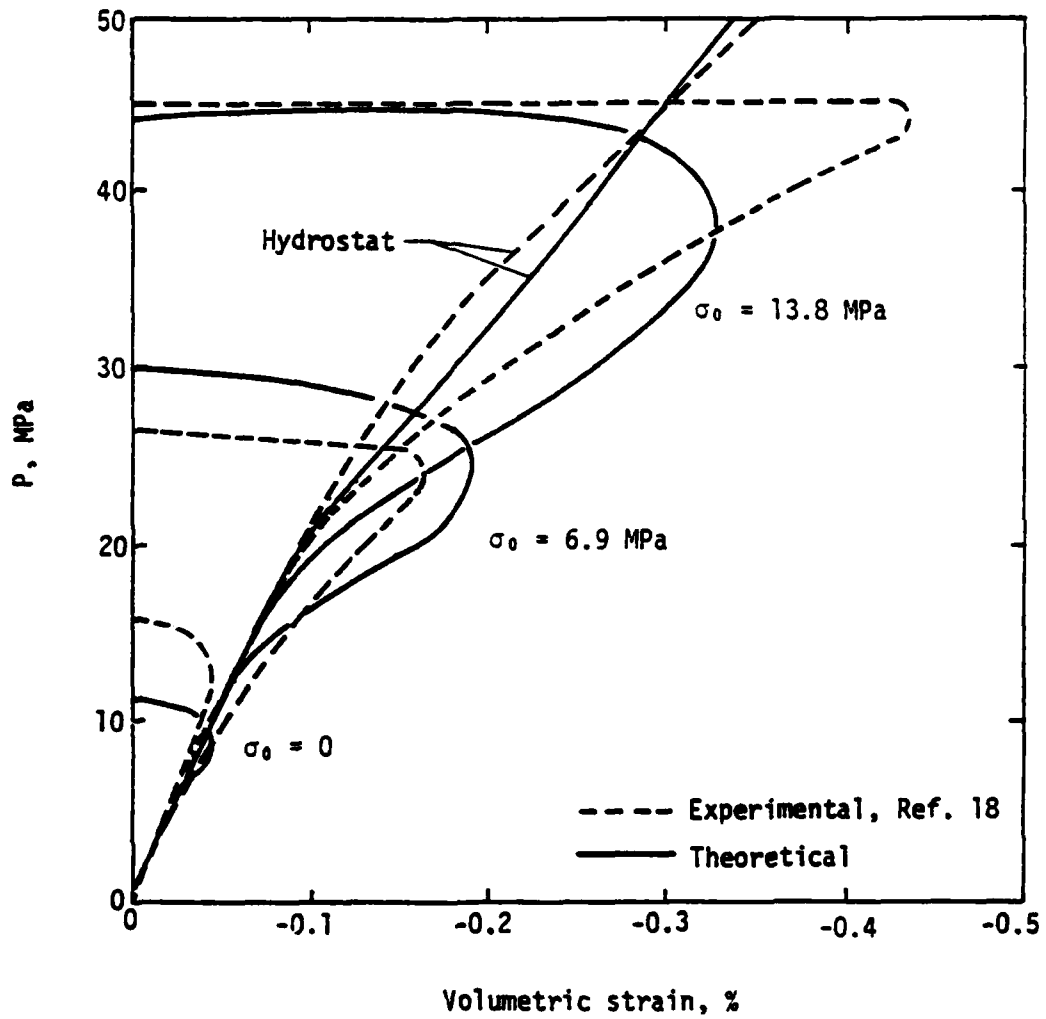
To demonstrate the flexibility of the model two materials with considerably different response characteristics were chosen. The first is a high-strength concrete that exhibits relatively little compaction but a considerable amount of dilatation. The second is a material similar to sand but with a large amount of porosity so that severe compaction but little dilatation is exhibited. For both cases, data were obtained from hydrostatic and triaxial compression tests. The plots of the triaxial results show stress and strain measured relative to σ_0 and ϵ_0 which denote the maximum value for stress and strain, respectively, obtained in the initial hydrostatic part of the path.

Results for the high-strength concrete tested by Green and Swanson [18] are shown in Figure 5 with the following material parameters used for predictions:

$$\begin{array}{lll} E = 35,000 \text{ MPa (Young's Modulus)} & & \nu = 0.25 \text{ (Poisson's ratio)} \\ \gamma_0 = 1.57 & & \gamma_L = 0.80 \\ \sigma_s = 3.7 \text{ MPa} & \epsilon_0^{-1} = 0.055 & n = 0.30 \\ b_1 = 0.35 & b_2 = 4.0 & b_3 = 2.0 \end{array}$$

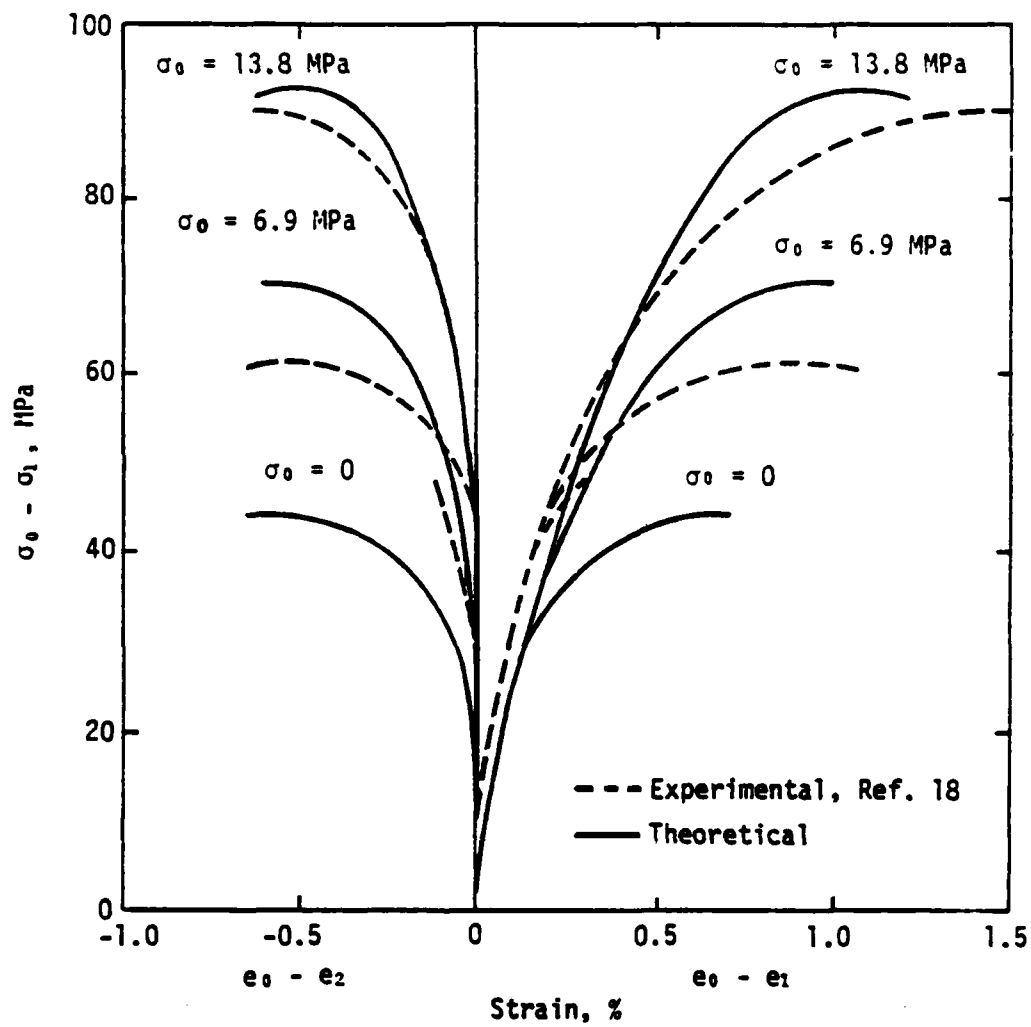
Plots of mean pressure versus volumetric strain in Figure 5a show both shear enhanced compaction and dilatation. Too much dilatation is predicted for the uniaxial stress path and the discrepancy is even greater on the plot of stress versus strain shown in Figure 5b. This is a consequence of using the measure, ϵ_0^{-1} , for all limit states. Predictions for the other paths are quite reasonable.

The second example involves foundry core which was first proposed by Grady [22] as a material for simulating cemented sand with material data obtained by Waterways Experimental Station. Since the density is relatively



(a) Mean pressure versus volumetric strain.

Figure 5. Experimental and theoretical response curves for a high-strength concrete.



(b) Stress versus strain.

Figure 5. Concluded.

low (1460 kg/m^3), Forrestal proposed a modification to the method of sample preparation which raised the density to 1820 kg/m^3 . This density is similar to that of dry porous tuff at the Sandia Tonapah Test Range where densities range from 1620 to 2000 kg/m^3 . The experimental data given here were obtained by Terra Tech [23] for pressures up to 400 MPa on material prepared at the Sandia National Laboratory foundry. Porosity was 30 percent. Material properties used for predictions are given as follows:

$$\begin{array}{lll}
 E = 1090 \text{ MPa} & & \nu = 0.22 \\
 \gamma_0 = 1.06 & & \gamma_L = 0.92 \\
 \sigma_s = 1.5 \text{ MPa} & \bar{e}_0^{-1} = 0.55 & n = 1.6 \\
 b_1 = 0.15 & b_2 = 0 & b_3 = 3.5
 \end{array}$$

The experimental results shown in Figure 6 are composite curves from two or more tests with difference bars shown to indicate the extent of variation that was observed among samples. Some of the difference between experimental and theoretical results in Figure 6a is due to the restriction imposed by the functional form of Eq. (9). Part of the discrepancies for the triaxial response paths of Figure 6b can be attributed to the use of the strain invariant \bar{e}^{-1} and the assumption that the limit state is reached at the same value of \bar{e}^{-1} no matter what path is followed. However the results are certainly adequate for engineering analysis since the variation in field properties is considerably more than that displayed by these test samples. Overall, correct response features are displayed with a rather elementary model for an extremely compressible material.

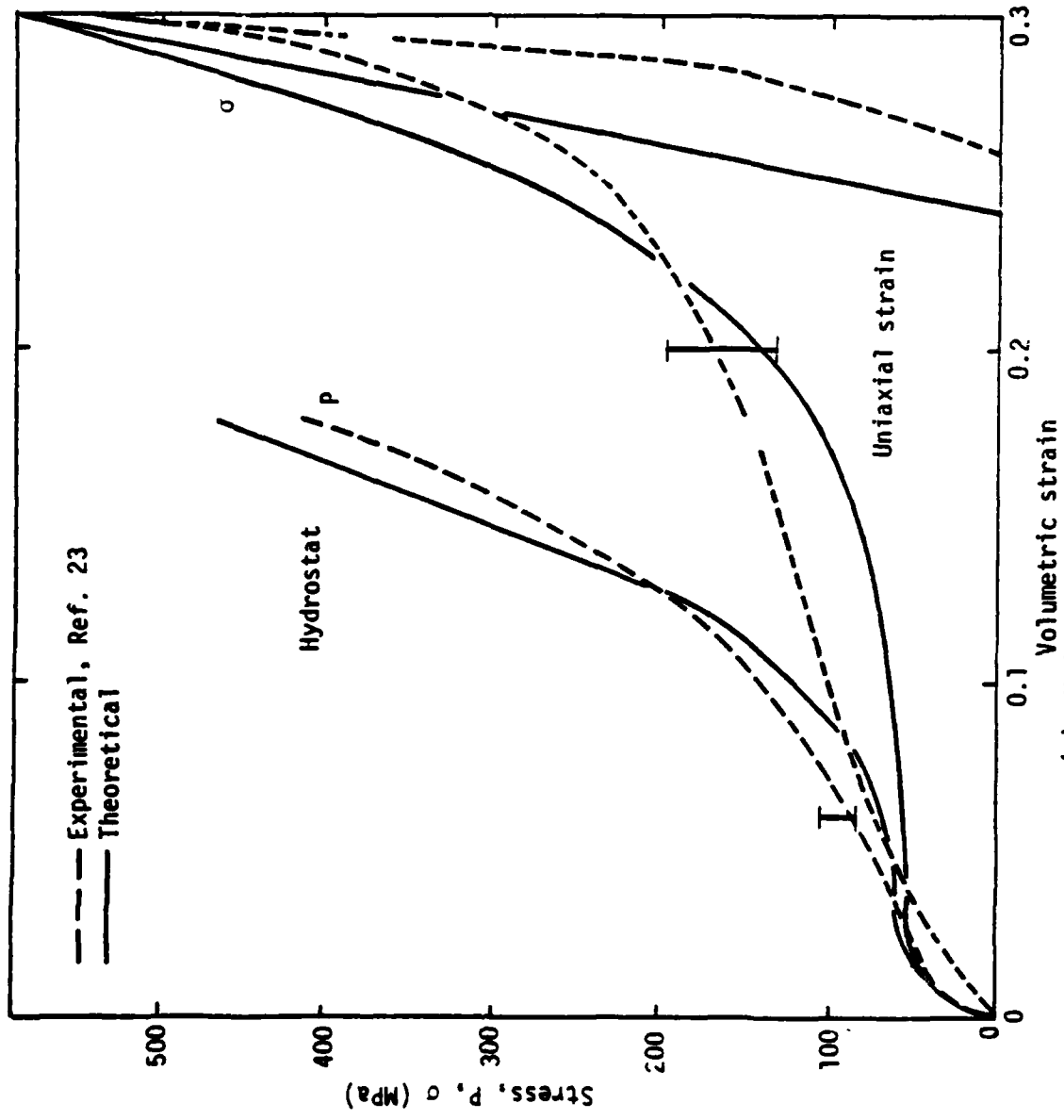
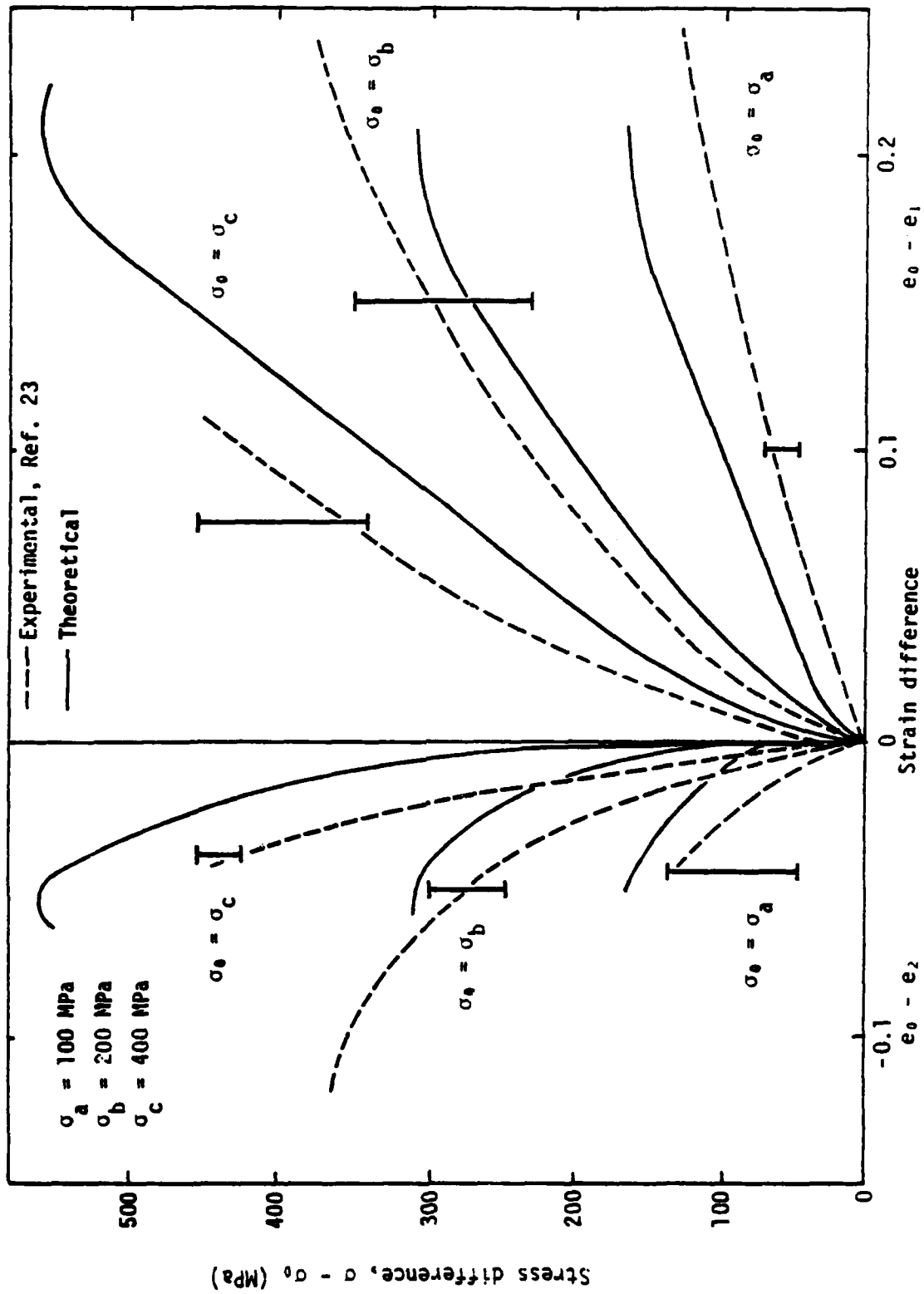


Figure 6. Experimental and theoretical response curves for a cemented sand.
 (a) Hydrostat and uniaxial strain.



(b) Stress versus strain. Figure 6. Concluded.

5. CONCLUDING REMARKS

This theory has been developed under rather restrictive conditions. Only paths defined by monotonically increasing stress or strain for positive mean pressure have been considered. Cyclic and rate effects have not been included although it is readily apparent that kinematic hardening and a rate sensitive flow surface can be incorporated in the theory.

This is one of a large number of investigations concerning the application of plasticity theory to frictional materials. However, in many instances the complexity of the models precludes their use for analysis and even for numerical computations. Since frictional materials are notorious for displaying experimental data with large scatter and for being extremely inhomogeneous in the field, it makes no sense from an engineering viewpoint to attempt to refine a model just to provide a close match to experimental data for all stress paths. In the same context, however, for general applications it is certainly necessary to have the capability for predicting correct response features which include shear enhanced compaction, dilatation, hardening, and softening. The actual degree of refinement that is required is a matter of judgement based on the particular application.

The initial workers in this field, as exemplified by the work in References 1 and 2, were attacking essential problems with a minimum degree of complexity. It is in this spirit that this model has been developed. The fundamental concepts are not new. By using stress invariants the theory is completely general and satisfies the principle of material frame indifference. By eliminating the second invariant, the theory is simplified considerably but essential response characteristics are still predicted. Fundamental features such as the limit state and the K_0 condition are displayed inherently by the model. Compaction and dilatation are controlled by the

parameter γ^* in the nonassociated flow rule while hardening and softening are controlled with γ . Some familiarity with the P-L space leads to natural interpretations that are in accord with experiment.

To the limited extent that the theory provides a natural description of physical phenomena using the clearest mathematical structure, this paper is offered as an expression of gratitude to Professor E. F. Masur, who has provided numerous examples of elegant research for others to emulate.

ACKNOWLEDGEMENT

This research was supported by the Air Force Weapons Laboratory and the Air Force Office of Scientific Research. S. Babcock and J. Bean provided invaluable assistance in assessing and testing the model under various stages of development.

REFERENCES

1. D. C. Drucker and W. Prager, "Soil Mechanics and Plasticity Analysis of Limit Design," Quarterly of Applied Mathematics, 10: 157-165 (1952).
2. D. C. Drucker, R. E. Gibson, and D. J. Henkel, "Soil Mechanics and Work-Hardening Theories of Plasticity," Transactions of the ASCE, 122: 338-346 (1957).
3. G. Y. Baladi and B. Rohani, "Elastic-Plastic Model for Saturated Sand," Journal of the Geotechnical Engineering Division, ASCE, 105: 465-480 (1979).
4. K. J. Willam and E. P. Warnke, "Constitutive Model for the Triaxial Behavior of Concrete," International Association of Bridge and Structures Subjected to Triaxial Stresses, Paper III-1, Bergamo, Italy, May 17-19, 1974.
5. P. V. Lade, "Elasto-Plastic Stress-Strain Theory for Cohesionless Soil with Curved Yield Surfaces," International Journal of Solids and Structures, 13: 1019-1035 (1977).
6. Vermeer, P. A., "A Double Hardening Model for Sand," Geotechnique, 28: 413-433 (1978).

7. Z. Mroz, V. A. Norris, and O. C. Zienkiewicz, "Application of an Anisotropic Hardening Model in the Analysis of Elasto-Plastic Deformation of Soils," Geotechnique, 29: 1-34 (1979).
8. S. S. Hsieh, E. C. Ting, and W. F. Chen, "A Plastic-Fracture Model for Concrete," International Journal of Solids & Structures, 18: 181-197 (1982).
9. R. D. Krieg, "A Practical Two Surface Plasticity Theory," Journal of Applied Mechanics, 42: 641-646 (1975).
10. Y. F. Dafalias and E. P. Popov, "A Model of Nonlinearly Hardening Materials for Complex Loading," Acta Mechanica, 21: 173-192 (1975).
11. J. H. Prevost, "Plasticity Theory for Soil Stress-Strain Behavior," Journal of the Engineering Mechanics Division, ASCE, 104: 1177-1194 (1978).
12. K. Hashiguchi, "Constitutive Equations of Elastoplastic Materials With Elastic-Plastic Transition," Journal of Applied Mechanics, ASME, 47: 266-272 (1980).
13. M. D. Coon and R. J. Evans, "Recoverable Deformation of Cohesionless Soils," Journal of the Soil Mechanics and Foundations Division, ASCE, 97: 375-391 (1971).
14. D. Kolymbas, "A Rate-Dependent Constitutive Equation for Soils," Mech. Res. Comm., 4(6): 367-372, 1977.
15. R. O. Davis and G. Mullenger, "A Rate-Type Constitutive Model for Soil with a Critical State," International Journal for Numerical and Analytical Methods in Geomechanics, 2: 255-282 (1978).
16. P. V. Lade and J. M. Duncan, "Cubical Triaxial Tests on Cohesionless Soil," Journal of the Soil Mechanics and Foundations Division, ASCE, 99: 793-812 (1973).
17. P. V. Lade, "Three-Parameter Failure Criterion for Concrete," Journal of the Engineering Mechanics Division, ASCE, 108:850-863 (1982).
18. S. J. Green and S. R. Swanson, Static Constitutive Relations for Concrete, AFWL-TR-72-244, Air Force Weapons Laboratory, Kirtland Air Force Base, New Mexico (1973).
19. L. A. Traina, Experimental Stress-Strain Behavior of a Low-Strength Concrete Under Multiaxial States of Stress, Report prepared for Air Force Weapons Laboratory, Kirtland Air Force Base, New Mexico (May 1982).
20. P. N. Michelis, "Work-Softening and Hardening Behavior of Granular Rocks," Rock Mechanics, 14: 187-200 (1981).

21. P. V. Lade and H. M. Musante, "Three-Dimensional Behavior of Remolded Clay," ASCE Journal of the Geotechnical Engineering Division, 104: 193-209 (1978).
22. M. J. Forrestal and D. E. Grady, "Penetration Experiments for Normal Impact into Geological Targets," International Journal of Solids & Structures, 18: 229-234 (1982).
23. R. H. Smith, Testing Program on Tamped Foundry Core, Letter report to M. J. Forrestal, Terra Tek, Salt Lake City, Utah (December 15, 1981).

END

FILMED

5-83

DTIC